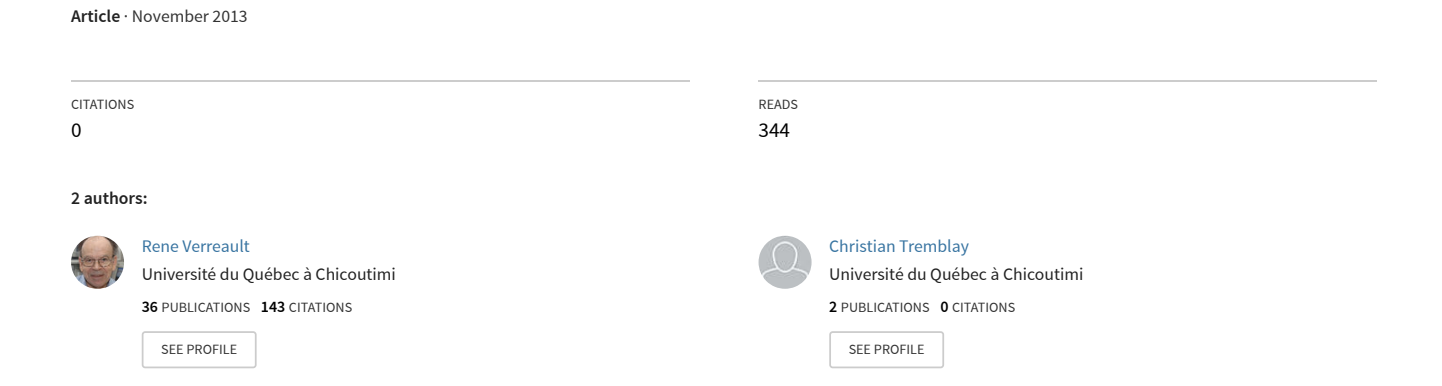
Characterizing the damping and the suspension anisotropy of a computerized Foucault pendulum



Characterizing the Damping and the Suspension Anisotropy of a Computerized Foucault Pendulum

René Verreault, Christian Tremblay

Université du Québec à Chicoutimi 555, boul. de l'Université, Saguenay, Québec, Canada G7H 2B1 rverreau@uqac.ca; christian@robotomation.ca

Abstract - All unsustained physical pendula undergo various types of damping processes which make them irreversible quasi-periodical devices. Their recent use as instruments for detecting cosmological micro-anomalies requires the determination of system anisotropy with the utmost precision, notwithstanding an inherent variance due to the strictly aperiodical behavior. An image processing algorithm has been developed for analyzing a camera monitored Foucault pendulum. This greatly improves precision in the determination of swinging azimuth, precession angle, swinging amplitude and swinging period. A novel, very simple damping formula has been derived based on sequential, instead of concomitant, viscous and aerodynamic damping processes within the oscillation cycle. Its high accuracy enables the authors to isolate a faint, undamped residual amplitude wave due to energy exchange between the minor and major axes of the elliptical orbit. To the authors' knowledge, the very weak anisotropy of a long Foucault pendulum has also been for the first time experimentally characterized in terms of the zero-amplitude swinging period plus a conservative wave in period as well as in amplitude.

Keywords: Physical pendulum, Foucault pendulum, viscous damping, aerodynamic drag, anisotropy, image processing.

1. Introduction

The simple pendulum is idealized in practically all textbooks as a harmonic oscillator obeying conservative Hamilton's mechanics. However, the mere presence of some inevitable damping in a physical pendulum prevents the trajectory in phase space from being closed and periodical. To address the damping phenomenon with classical conservative perturbation methods, the phase space trajectory is made artificially closed by making the energy loss over one half-cycle stored in some imaginary potential reservoir, and then given back to the pendulum in a time reversal process for the next half-cycle, thus preserving the Hamiltonian description (Minorsky, 1962). The Foucault pendulum has been thoroughly investigated by Nobel Prize Kamerlingh Onnes (1879) in his dissertation, where it was idealized as a two-degrees-of-freedom harmonic oscillator. Kamerlingh Onnes was the first to apply the perturbation methods of celestial mechanics to the spherical pendulum. His main contribution was to show, theoretically and experimentally, that the natural tendency of the spherical pendulum to generate elliptical orbits within a few minutes of operation was largely due to suspension anisotropy. Some 200 years after Foucault, the French engineer and Nobel Prize Maurice Allais (1959, 1997, 1999 and Web-1) designed the so-called paraconical pendulum with rolling ball suspension. Allais characterized the amount and orientation of pendulum anisotropy by the initial rate of increase of the ellipse minor axis and by the rate of Airy precession over 14 minutes. Beside suspension anisotropy, he detected an unidentified, variable source of anisotropy which he attributed to space, since it was correlated with the motion of particular celestial bodies in the solar system.

Much concern about the Foucault pendulum as a scientific instrument has been revived in the last 50 years. See Verreault (2013) for a short review. However, researchers are facing several drawbacks due to the irreversible, non-reproducible nature of the experiments. Namely, physical pendula show a non-negligible 3rd degree of freedom (Verreault, 2011) in the form of a torsion about the suspension wire or rod axis (some sort of macroscopic spin degree of freedom), which takes part in the repartition of energy and momentum. Moreover, every physical pendulum with swinging amplitudes of a few centimetres undergoes prevalent aerodynamic damping with different power loss parameters for each degree of freedom. Finally, nonlinear coupling can also cause conservative energy transfer between the degrees of freedom.

In view of the recent interest in the spherical pendulum as a cosmological anisotropy measuring instrument, it is the purpose of this paper to show how, by using appropriate image processing algorithms, and irrespectively of the various dissipative processes, 1° a conservative energy transfer between the pendulum proper modes can be experimentally demonstrated; 2° the zero-amplitude swinging period can be precisely determined for each azimuth and used to characterize the pendulum anisotropy.

2. Theoretical background

2.1 The period of oscillation

While the scientific literature generally considers the Foucault pendulum as a two-dimensional harmonic oscillator, it must be emphasized that it is virtually impossible to set up a perfectly isotropic physical pendulum. Fundamentally, suspension anisotropy arises as a consequence of a varying effective length of the pendulum as a function of swinging azimuth. Therefore, two extreme values of swinging period can be measured for two orthogonal directions, namely the fast axis (minimal period) and the slow axis (maximal period). The work of Kamerlingh Onnes (1879) on suspension anisotropy established that, in absence of anharmonicity, the initial rate of increase of the minor axis, shortly after the pendulum has been launched in a rectilinear oscillation, can be a measure of the amount of suspension anisotropy.

$$\dot{\varepsilon} = A \sin 2\psi_0 \tag{1}$$

where

 $\varepsilon = b/a$, the ellipse axis ratio;

A is the measure of the amount of anisotropy;

 ψ_0 is the initial azimuth of the rectilinear oscillation relative to fast axis.

Allais (1959) utilized, in his mid-fifties experiments, an anisotropic Foucault pendulum by design, partly due to a disk shaped bob lying in a vertical plane, partly due to a suspension rod terminated at the top by a C-shaped stirrup and partly due to the anisotropic elastic constants of a steel beam, near the ceiling, supporting the suspension rig. Moreover, his short pendulum (~1 m) with large amplitudes (~0,1 rad) was strongly nonlinear, so that the Airy precession rate which accompanied the elliptical orbit build-up reached typically twice the negative of the Foucault rate after 14 minutes. As a matter of fact, Allais also used the Airy precession rate as the measure of pendulum anisotropy, since it included the integral of Equation 1 over 14 minutes (Allais 1997).

For a long Foucault pendulum at mid-latitudes with amplitudes in the range 0.001- 0.015 rad, Airy precession is generally negligible, while Foucault precession is dominant. However, the effects of even very little suspension anisotropy are not negligible if the experiment is to be conducted over several hours. An efficient but not so accurate method of determining suspension anisotropy may consist in a series of direct measurements of the swinging period T for a set of evenly spaced swinging azimuths over a small number of oscillations (typically 100 cycles). By fitting a sine wave to the data, the amount of anisotropy is obtained as

$$\Delta\omega = \omega_{max} - \omega_{min} = -(T_{max} - T_{min})/T_0^2, \quad (\omega = 2\pi/T)$$
 (2)

In the same process, the azimuths of the fast and slow axes can be determined.

Since 2001, the first author has conducted several Foucault pendulum runs lasting from 12 to 36 hours. Thanks to Foucault precession, a large range of swinging azimuths is then visited as a function of

time. It becomes possible in aftermath to extract the period time series. After eliminating a transient contribution T_{γ} due to the anharmonic influence of finite swinging amplitudes, the remaining "zero amplitude" series should fit a Fourier series with a fundamental component at one half (noted T_F) of the Foucault precession period, since each swinging azimuth is visited twice during a complete revolution in precession. As shown by Kamerlingh Onnes (1879), suspension anisotropy is responsible for its own precession contribution, even in the absence of Airy effect. Consequently, the precession rate is by no means constant, which should show up as a significant harmonic content in the above time series. The swinging period should then be expressed as

$$T(t) = T_0 + T_{\gamma} e^{-t/\gamma} + \sum_{k=1}^{n} T_k \cos\left(\phi_k + \frac{2\pi kt}{T_E}\right).$$
 (3a)

However, if the independent variable is the azimuth of the major axis instead of the time, the swinging period $T(\psi)$ should show a similar behaviour as T(t), but only with the fundamental Fourier component, since the precession lead and lag no longer show up. The transient period increment should essentially be the same but logarithmic decrement will be parametrized by an azimuth constant δ . Hence,

$$T(\psi) = T_0 + T_{\gamma} e^{-t/\delta} + T_1 \cos\left(\phi_1 + \frac{2\pi t}{T_F}\right). \tag{3b}$$

2.2 The damping

In Equation 3, the transient term is related to the steadily decreasing major axis due to aerodynamic and viscous damping. Considering the simultaneous average dissipative work done against the viscous forces and the aerodynamic forces during one half-oscillation, Nelson (1986) comes up with the differential equation

$$\dot{a} = -\alpha a - \beta a^2,$$

which, upon integration, gives

$$a = \frac{\alpha a_0 e^{-\alpha t}}{\left\lceil \beta a_0 \left(1 - e^{-\alpha t} \right) + \alpha \right\rceil}.$$
 (4)

However that expression proved erroneous by more than 100% for runs exceeding 12 hours. Taking into account the constantly varying speed of the bob within a half-cycle, a small fraction of the half-cycle has Reynolds numbers between 0 and 1000 with negligible aerodynamic drag, while the remaining fraction has Reynolds numbers well above 1000 (typically in the 3000-10000 range) with negligible viscous damping. Then, the linearly damped amplitude at the end of the slow cycle fraction can be considered as the starting amplitude at the beginning of the following rapid fraction. Applying perturbation methods (Minorsky 1962) to this principle, a much simpler novel expression is obtained, which has been found to fit the data within the experimental errors of amplitude (typically 10 to 15 μ m) for runs reaching up to 18 hours:

$$a = \frac{a_0 e^{-\alpha t}}{\left(1 + \beta a_0 e^{-\alpha t}t\right)} = \frac{a_0}{\left(e^{\alpha t} + \beta a_0 t\right)},$$
(5)

where

 $1/\alpha$ is the viscous time constant, and

 $1/\beta a_0$ is some kind of aerodynamic time constant.

2.3 The intermode energy exchange

It is expected that the vibration energy along the minor axis, as anisotropy generates ellipses, is extracted from the major axis. Since suspension anisotropy effects involve the half-Foucault precession period T_F , a Fourier series similar to the one of Equation 3a should be present in the amplitude of the major axis as well, although, to the authors' knowledge, such fluctuations in the amplitude curve have never been reported in modern Foucault pendulum experiments. At most, with the excessively anisotropic pendulum used by Kamerlingh Onnes (1879) in his dissertation, the fatter ellipses drawn in his figures (see Figure 1 below) show evident reductions of the major axis. It is not clear at first glance whether and how that oscillatory contribution to the major axis amplitude is affected by dissipation since Kamerlingh Onnes did not consider damping. The different models to be tested may look as follows:

a) multiplificative dissipative anisotropy effects:

$$a(t) = \frac{a_0}{\left(e^{\alpha t} + \beta t\right)} \left(\sum_{k=1}^n a_k \cos\left(\phi_k + \frac{2\pi kt}{T_F}\right)\right); \tag{6}$$

b) additive dissipative anisotropy effects:

$$a(t) = \frac{a_0}{\left(e^{\alpha t} + \beta t\right)} + \sum_{k=1}^{n} \frac{a_k}{e^{\gamma_k t}} \cos\left(\phi_k + \frac{2\pi kt}{T_F}\right); \tag{7}$$

c) additive conservative anisotropy effects:

$$a(t) = \frac{a_0}{\left(e^{\alpha t} + \beta t\right)} + \sum_{k=1}^{n} a_k \cos\left(\phi_k + \frac{2\pi kt}{T_F}\right). \tag{8}$$

Which one is the correct model should be decided by curve fitting to the experimental data.

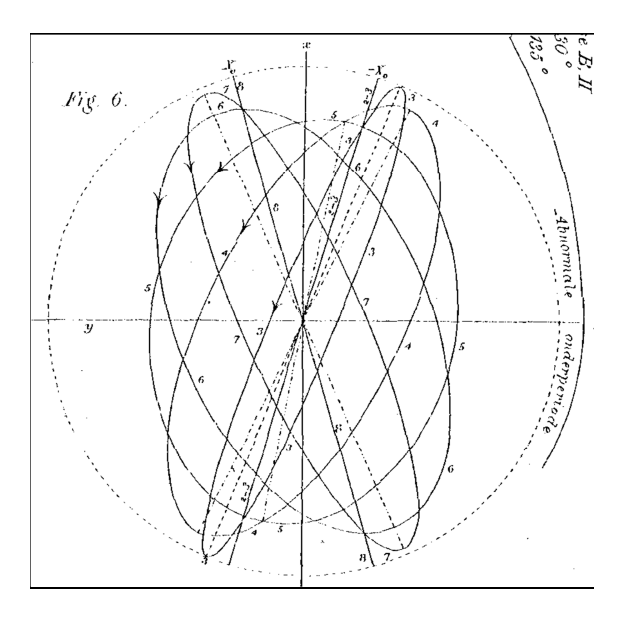


Figure 1. Reproduction of Figure 6 from Kamerlingh Onnes' dissertation. From energy conservation principle, the fatter the ellipses (v.g. Nos 5 and 6), the shorter the major axis as compared to the rectilinear oscillation (No 8).

2.4 The anharmonicity

For an isotropic pendulum, the finite amplitude of oscillation is responsible for a period increment according to the expression

$$T(t) = T_0 \sqrt{1 + \frac{a^2(t)}{8l^2}} \approx T_0 \left(1 + \frac{a_0^2}{16l^2 \left(e^{\alpha t} + \beta a_0 t \right)^2} \right) \qquad (a_0 \ll l)$$
 (9)

where

 T_0 is the zero-amplitude period;

l is the pendulum length.

For the first few hours, an approximation to the transient term can be given by

$$T(t) \approx T_0 \left(1 + \frac{a_0^2}{16l^2 \left(1 + 2(\alpha + \beta a_0)t + \dots \right)} \right) \approx T_0 + T_{\gamma} e^{-2(\alpha + \beta a_0)t} \qquad (t < 1/\alpha < 1/\beta a_0) \quad (10)$$

where, by comparing with Equation 3a,

$$T_{\gamma} \approx \frac{T_0 a_0^2}{16l^2} \quad ; \tag{11}$$

$$1/\gamma \approx 2(\alpha + \beta a_0). \tag{12}$$

3. Experimental setup

The data used for this research originates from an 8 m Foucault pendulum set up in Gifu, Japan, for the solar eclipse of July 22, 2009 (Web-2). The experimental site consisted of a white concrete bunker 15m x 13m x 8.5m on the University campus. The suspension rig was clamped to a 19mm U-bolt emerging from a ceiling concrete beam. A Watec 902-H2 video camera was horizontally fixed to the suspension rig so as to get a parallax-free vertical view of the pendulum bob, though a pair of mirrors at 135° to each other. The 18-hour continuous recording at 30 frames per second fills up a 1.5 terabyte hard disk. The positions of the bob and of the reference alidade are made visible through a set of retro-reflecting markers which are illuminated from a small spotlight located near the suspension rig.

In order to achieve the maximum available precision from the data processing, proprietary software has been developed. In a pre-processing phase, a listing of the coordinates of the retro-reflecting markers is made. Then a quarter of ellipse is fitted to each quarter of a cycle, in order to determine the major and minor axes twice per cycle. Moreover, two period calculations per cycle are made by comparing the times of passage at the end of the major and minor axes between consecutive cycles. To make those period measurements comparable with those of the literature, which typically are averages over ~100 cycles, a running mean has been applied over 85 cycles trough out the data. In this manner, any unknown effects originating from accidental torsional spinning motion of the bob with an observed spin period of 85 swing cycles are eliminated.

From the theory standpoint (Kamerling Onnes, 1979), the different longwise and crosswise elastic properties of the rig and beam assembly generate two distinct periods for swinging directions parallel and perpendicular to the beam. Hence, linear anisotropy manifests itself as a tendency for the rectilinear oscillations in the intermediate quadrants to degenerate into elliptical orbits. A complete cycle of period values should thus be observed over a 180° azimuth span. Since that azimuth interval is normally scanned, due to the Foucault precession, in one half of the Foucault period, it is expected that the anisotropy features shall be expressed as a Fourier series with the half-Foucault period ($T_F = 20.68 \text{ h}$) for the fundamental component.

Among the aims of this research, while all sorts of external perturbations, particularly during solar eclipses, also tend to induce elliptical orbits, it is important to precisely characterize the amount of

ellipticity originating from suspension anisotropy. For this work, only the evolutions of the swinging amplitude and of the swinging period over the 18-hour duration of the experiment have been considered.

4. Results and discussion

Figure 2 shows the evolution of the amplitude. The actual graph consists of 19 803 experimental points which are measured with an accuracy of 15 μm rms. This provides enough information to determine not only the viscous and aerodynamic damping parameters, but also a 3-harmonic Fourier series at the half-Foucault fundamental period corresponding of the energy exchange between the major and minor axes when the latter grows up due to suspension anisotropy. It can be verified that the maximum of the minor axis of Figure 2 coincides with the minimum of the fundamental wave of the major axis. Here, it is worth noting that the huge amount of redundant information available in video imagery allows unprecedented precision in the determination of the pendulum characteristics of Table 1. In particular, the novel damping law as per Equation 5 is exactly verified within experimental errors for the complete duration of the 18-hour experiment. Regarding the anisotropy models of Equations 6 to 8, attempts to fit any dissipative model lead to inconclusive results. On the contrary, the conservative model yielded the consistent results of Table 1 within the experimental errors.

In Figure 3, the three synchronized waves characterizing the anisotropy effects on the major axis, the minor axis and the swinging period are quite well illustrated.

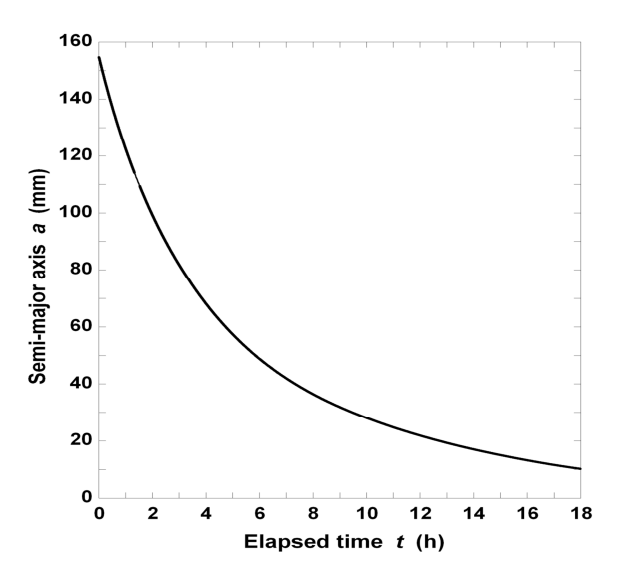


Fig. 2. Swinging amplitude as a function of time. The available information allows the significant determination, in addition to the viscous time constant α^{-1} and the aerodynamic "time constant" $(\beta a_0)^{-1}$, of a 3-harmonics periodical part describing the conservative energy exchange between the minor and major axes according to the anisotropy tendency to generate a minor axis wave at half the Foucault precession period, namely 20.68 h in Gifu.

Table 1. Parameters pertaining to a fit of Equation 5 to the amplitude data of Figure 1.

Parameter		Value	Standard error
a_0	(mm)	154.356	0.003
1/α	(h)	6.6517	0.0006
$1/\beta a_0$	(h)	10.065	0.004
a_1	(mm)	1.307	0.002
$arphi_1$	(rad)	1.392	0.002
a_2	(mm)	0.3049	0.0006
φ_2	(rad)	6.011	0.002
a_3	(mm)	0.0386	0.0003
φ_3	(rad)	4.809	0.006
Residuals (mm)		0.015	

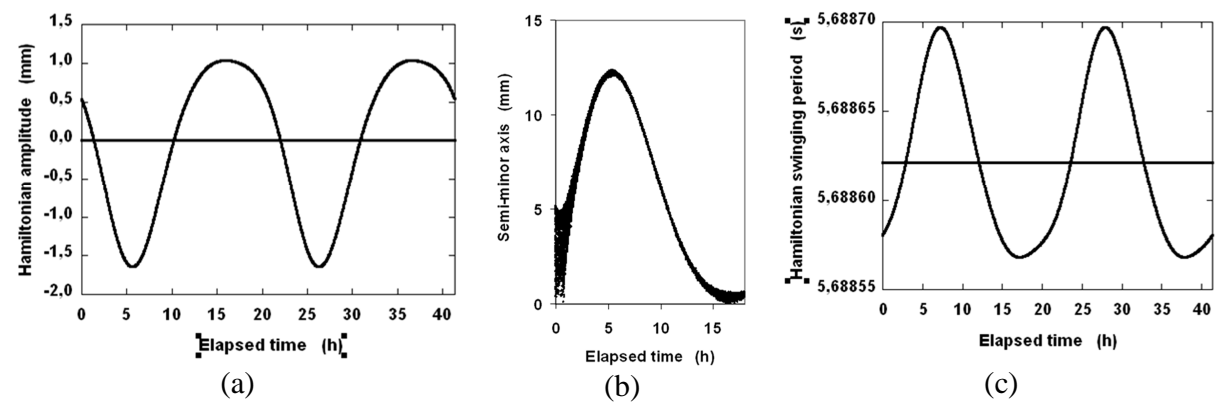


FIGURE 3. (a) Evolution of the Hamiltonian, energy conserving amplitude wave of the semi-major axis, unaffected by the damping processes, due to the energy taken by the semi-minor axis. (b) Evolution of the ellipse semi-minor axis as a consequence of the azimuth dependence of the period due to suspension anisotropy. (c) Evolution of the zero-amplitude Hamiltonian swinging period, unaffected by the damping processes, for a complete Foucault precession period of 41.36 h.

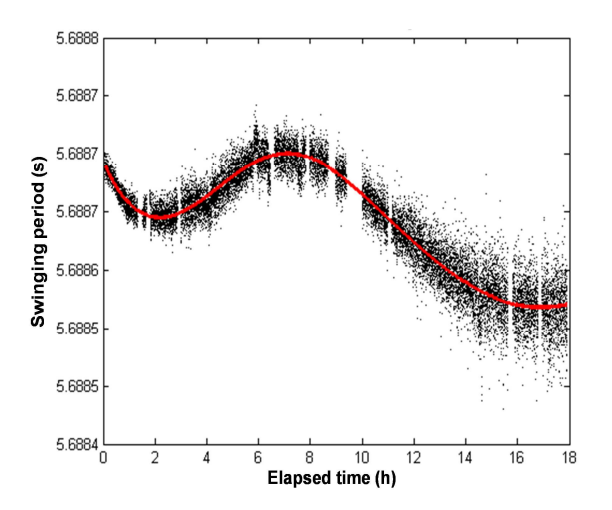


Figure 4. Evolution of the swinging period as a function of time.

Table 2. Parameters pertaining to a fit of Equation 3 to the swinging period data of Figure 4.

Parameter		Value	Standard error
T_0	(s)	5.6686215	0.0000004
T_{γ}	(s)	0.0001198	0.0000011
γ	(h)	1.72	0.05
T_1	(s)	0.0000658	0.0000002
φ_1	(rad)	4.03	0.01
T_2	(s)	0.0000103	0.0000003
φ_2	(rad)	2.02	0.02
T_4	(s)	0.0000017	0.0000001
$arphi_4$	(rad)	4.22	0.08
Residuals	(s)	0.000012	

Figure 4 and Table 2 illustrate the adjustment of Equation 3a to the swinging period time series. As expected, the important harmonic content could be anticipated, since precession acceleration or deceleration would cause leads or delays in the instant where the major axis azimuth crosses the anisotropy fast and slow axes. Another test of the above anisotropy theory consists in the verification of the link (Equations 11 and 12) between the transient period pattern and the anharmonicity parameters, as shown in Table 3.

Table 3. Experimental verification of anharmonicity parameters with Equations 11 and 12.

Parameter	Theoretical estimate	Experimental value
T_{γ} (µs)	131	120
1/γ (h ⁻¹)	0.58	0.50

Figure 5 shows the experimental results for the evolution the swinging period as a function of swinging azimuth. Again, the 19 803 data points show an average residual of 14 μs. Therefore, only two contributions to the mean period are neatly separated: a) transient addition to the ideal zero-amplitude period, with a damping azimuth constant of 17.1°; b) a sinusoidal zero-amplitude period which verifies exactly the theory of anisotropy according to Equation 3b. In further processing of the pendulum data, it is then possible to exactly predict the amount of precession rate attributed to the linear anisotropy of suspension, so that any amount there upon will have to be attributed to external perturbations.

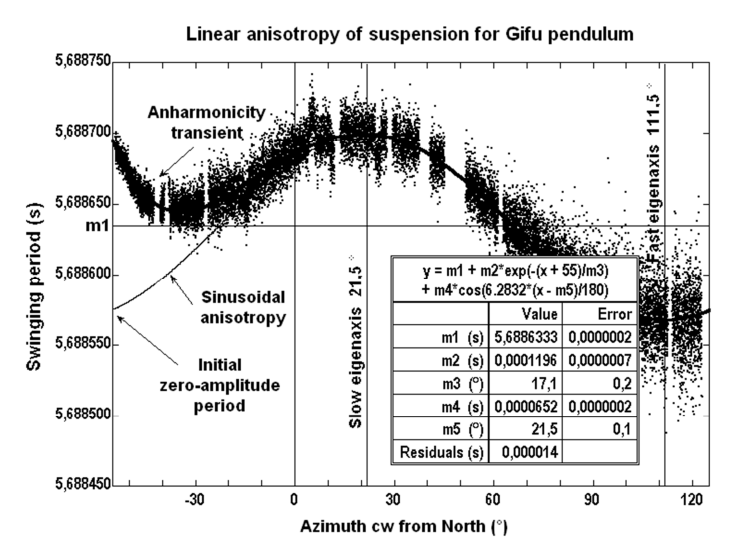


Fig. 5. Linear anisotropy of suspension for the Gifu pendulum, expressed as a pure sine wave for the swinging period in terms of the swinging azimuth. The swinging period includes a transient contribution due to anharmonicity and proportional to the square of the swinging amplitude.

5. Conclusion

The combined use of video imagery and proprietary software involving piecewise curve fitting over terabytes of data stream has allowed unprecedented precision in the determination of the Foucault pendulum parameters. To the authors' knowledge, the weak suspension anisotropy of a long Foucault pendulum has been experimentally determined for the first time in terms of period measurements with sub-microsecond precision. Moreover, a novel damping theory which discriminates between the linear and quadratic processes within the oscillation cycle appears to be the sole description capable of reproducing the experimental measurements over an 18-hour long experiment.

Acknowledgements

The first author is profoundly indebted to Mr Thomas J. Goodey for beneficial discussions and for technical assistance in designing the experiment. Moreover, the dedicated efforts of Professor Kazuo Tanaka, Gifu University, for providing the high quality experimenting site are gratefully acknowledged.

References

Allais M. (1959), Should the laws of gravitation be reconsidered? Part II – Experiments in connection with the abnormalities noted in the motion of the paraconical pendulum on an anisotropic support, Aero/Space Engineering, 18, No 10, 55-59 and No 11, 55.

Allais M. (1997), L'anisotropie de l'Espace, Clément Juglar, Paris, p.243.

Allais M. (1999), The "Allais effect" and my experiments with the paraconical pendulum 1954-1959, a Memeoir prepared for NASA, 84 p, downloadable from Web-1.

Kamerlingh Onnes H. (1879), "Nieuwe Bewijzen voor de Aswenteling der Aarde", Ph.D. Thesis, Rijksuniversiteit te Groningen, Groningen, NL, , (in Dutch). "New Proofs of the Rotation of the Earth", Partial Translation by V. O. de Haan in: "Should the Laws of Gravitation Be Reconsidered?", edited by H. A. Munera, Montreal: Apeiron, 2011, pp. 425-447.

Minorsky N. (1962), "Nonlinear Oscillations", Princeton: D. van Nostrand, p. 330.

Nelson R. (1986), The pendulum – Rich physics from a simple system, Am. J. Phys. 54, 112-121.

Verreault R. (2011), Tidal Accelerations and Dynamical Properties of Three-Degrees-of-Freedom Pendula, in "Should the Laws of Gravitation Be Reconsidered?", edited by H. A. Munera, Montreal: Apeiron, pp. 111-126.

Verreault R. (2013), Can gravitation anisotropy be detected by pendulum experiments? Journal of Computational Methods in Sciences and Engineering 13, 279-290.

Web sites:

Web-1: http://www.allais.info/, consulted 11 April 2013.

Web-2: http://www.youtube.com/watch?v=vsygRYfubVY/, consulted 11 April 2013.